Ab initio investigation of the electronic structure and bonding of BH, BH⁻, and HBBH molecules

Evangelos Miliordos and Aristides Mavridis[a)]
Laboratory of Physical Chemistry, Department of Chemistry, National and Kapodistrian University of Athens, P.O. Box 64004, Zografou, 157 10 Athens, Greece

By correlating all electrons and employing core-tuned correlation consistent basis sets of quintuple-ζ quality, we applied multireference and coupled-cluster methods to study 32 electronic states of the diatomic BH molecule, two bound states of BH⁻, and three states of the linear HBBH molecule. We have constructed full potential energy curves and profiles, reporting binding energies, geometries, spectroscopic parameters, dipole moments, and energy separations, whereas our numerical results are in excellent agreement with available experimental numbers. We are trying as well to interpret the binding modes of a large number of the examined states. 18 states of BH are of Rydberg character, with the BH⁻ anion revealing similar structural characteristics to the isoelectronic CH species. The first three states of HBBH $\widetilde{X} \, ^3\Sigma_g^-$, $\widetilde{a} \, ^1\Delta_g$, and $\widetilde{b} \, ^1\Sigma_g^+$ diabatically correlate to two $a \, ^3\Pi$ BH fragments, they are similar to the states $b \, ^3\Sigma_g^-$, $B \, ^1\Delta_g$, and $B' \, ^1\Sigma_g^+$ of the isoelectronic molecule C_2, however, their ordering follows that of the first three states of the O_2 molecule. © *2008 American Institute of Physics.* [DOI: 10.1063/1.2902284]

I. INTRODUCTION

We have studied the electronic structure of the diatomic BH, its anion BH⁻, and the dimmer B_2H_2 by *ab initio* multireference and coupled-cluster methods. With no doubt boron is one of the most interesting elements of the Periodic Table;[1] the bewildering geometrical, electronic, and structural variety of boranes, compounds made of boron and hydrogen (B_xH_y), is revealing of its complex, unique, and diverse chemistry.[2]

The diatomic boron hydride (BH), the simplest of boranes and of all stable diatomic molecules but H_2, LiH, and BeH, was first observed in 1931 by Lochte-Holtgreven and van der Vleugel who recorded the optically allowed $A \, ^1\Pi \leftarrow X \, ^1\Sigma^+$ and $b \, ^3\Sigma^- \leftarrow a \, ^3\Pi$ transitions at 433 and 370 nm, respectively.[3] A considerable number of experimental works followed, mainly on the seven states $X \, ^1\Sigma^+$, $a \, ^3\Pi$, $A \, ^1\Pi$, $b \, ^3\Sigma^-$, $C' \, ^1\Delta$, $B \, ^1\Sigma^+$, and $C \, ^1\Sigma^+$ within an energy range of about 7 eV. All available experimental results on BH are collected in Table I. Interestingly enough no definitive experimental binding energy for the $X \, ^1\Sigma^+$ state exists. As a matter of fact Huber and Herzberg[9] reported a D_0 value of 3.42 eV (=78.9 kcal/mol), derived from an experimental predissociation limit of the $A \, ^1\Pi \leftarrow X \, ^1\Sigma^+$ transition and after subtracting an estimated height of the potential hump (≈ 0.155 eV) in the $A \, ^1\Pi$ state (*vide infra*). A more accurate D_0 value was suggested by Johns *et al.*[11] who observed one more vibrational level ($\nu = 3$) of the $A \, ^1\Pi$ state, hence $D_0 = 28850 \pm 150$ cm⁻¹ (=82.5 ± 0.43 kcal/mol). However, Bauschlicher *et al.*,[12] after analyzing the tunneling through the barrier of the $A \, ^1\Pi$ state, proposed that "D_0 and the predissociation limit differ by about 0.8–0.9 kcal/mol," sug-

gesting finally $D_0 = 81.6 \pm 0.6$ kcal/mol. It is also noteworthy that the $a \, ^3\Pi$-$X \, ^1\Sigma^+$ energy separation has not yet been experimentally determined.

The first *ab initio* study on BH was published in 1956 by Shani.[13] Since then a large number of theoretical studies have been reported mainly on the *X*-state of BH. Clearly, the small size of the BH molecule is very attractive as a testing ground for the development of new electronic structure *ab initio* methods. Curtiss and Pople[14] through QCISD(T) calculations correlating all six electrons of BH obtained $D_0(X \, ^1\Sigma^+) = 81.5$ kcal/mol, whereas Bauschlicher *et al.*[12] confirmed this value at the MRCI level. The most accurate dissociation energy seems to be that of Feller *et al.*[15] who obtained $D_0 = 81.5$–81.7 kcal/mol at the CCSD(T)-complete basis set (CBS) limit level. Radiative life times of the spin-allowed $A \, ^1\Pi$-$X \, ^1\Sigma^+$ and $b \, ^3\Sigma^-$-$a \, ^3\Pi$ transitions have also been studied, the most recent works being that of Luh and Stwalley[16] and Pederson *et al.*[17] A large number of theoretical works have been devoted on the spectroscopic parameters of the seven experimentally well-known (see Table I) states of the BH molecule.[18] The most recent theoretical work seems to be that of Gagliardi *et al.*,[19] who constructed complete potential energy curves (PECs) of 20 electronic states at the full (valence) configuration interaction level, combined with a $[5s4p2d1f/_B \, 4s3p2d/_H]$ basis set. Numerical results are reported, however, only for the first six states; as we will see our results deviate considerably from those of Ref. 19. Finally, the static electric properties such as dipole moment (μ) and polarizability (α) of the ground state have been calculated by Waltz *et al.*,[20] Daborn and Handy,[21] and Halkier *et al.*,[22] whereas Jaszuński *et al.*[18(g)] determined μ and α of the $A \, ^1\Pi$ and $B \, ^1\Sigma^+$ states; the $\mu(X \, ^1\Sigma^+)$ values range from 1.30 (Ref. 21) to 1.73 (Ref. 22) D. Undoubtly the most accurate theoretical result is that of Ref. 22, $\mu_e(\mu_0) = 1.398(1.356)$ D

[a)]Author to whom correspondence should be addressed. Electronic mail: mavridis@chem.uoa.gr.

TABLE I. Existing experimental data of the ^{11}BH molecule. Equilibrium bond distances r_e (Å), spectroscopic parameters ω_e, $\omega_e x_e$, $\omega_e y_e$, a_e, γ_e, $\bar{D}_e$ (cm^{-1}), dipole moments μ(D), and energy separations T_0 (cm^{-1}). Spectroscopic parameters are defined through the relation $T(v,J)=\omega_e(v+1/2)-\omega_e x_e(v+1/2)^2$ $+\omega_e y_e(v+1/2)^3+\cdots+B_e J(J+1)-a_e(v+1/2)J(J+1)+\gamma_e(v+1/2)^2 J(J+1)+\cdots-\bar{D}_e J^2(J+1)^2-\beta_e(v+1/2)J^2(J+1)^2+\cdots+H_e J^3(J+1)^3+\cdots$, $B_e=h/8\pi^2 c\mu r_e^2$ (see Ref. [4]).

State	r_e	ω_e	$\omega_e x_e$	$\omega_e y_e$	a_e	γ_e	$\bar{D}_e(\times 10^3)$	μ	T_0
$X\,^1\Sigma^{+a}$	1.232 18	2366.728	49.338	0.3619	0.421 52	0.003 32	1.231		0
$X\,^1\Sigma^{+b}$		2364.657	47.710		0.421 59	0.003 35	1.2344	1.27 ± 0.21[c]	
$a\,^3\Pi^d$	1.200 6(=r_0)[e]	2625.1	55.8	−0.2	0.415 6	0.001 4	1.2348		x
$A\,^1\Pi$	1.218 6[e]	2251.458[f]	56.573[f]	−15.8295[g]	0.834 6[e]	0.132 2[g]	1.4557[b]		(T_e=)23 105.10[b]
		2342.413[b]	127.76[b]		0.537 7[f]	−0.100 8[b]		0.58 ± 0.04[c]	
$b\,^3\Sigma^{-d}$	1.227 1(=r_0)[e]	2438.10	55.56	−0.39	0.431	−0.006 7	1.258		x+27 152.5
$C'\,^1\Delta^e$	1.196 3	2610.02	46.62		0.390		1.219		(T_e=)45 981.0
$B\,^1\Sigma^{+e}$	1.216 4	2399.91	69.519	−3.927[g]	0.485	−0.042 4[g]	1.26		(T_e=)52 335.8
$C\,^1\Sigma^{+e}$	1.212 9	2474.72	54.424	0.228[g]	0.432		1.247		(T_e=)55 281.1
$D\,^1\Pi^e$	1.217 3(=r_0)						1.3		61 105.4
$E\,^1\Sigma^{+e}$									61 872.3
$F\,^1\Sigma^{+e}$									66 079.5
$G\,^1\Pi^e$	1.220 6(=r_0)								66 399.3
$H\,^1\Delta^e$									66 419.7
$I\,^1\Sigma^{+e}$	1.234(=r_0)								67 395.8
$J\,^1\Sigma^{+e}$									70 040
$K\,^1\Pi^e$									71 840

[a]Reference [5]. Fourier transform (FT) emission spectroscopy; these authors give also $\beta_e=-2.19\times 10^{-3}$ cm^{-1} and $H_e=0.87\times 10^{-7}$ cm^{-1}.
[b]Reference [6]. Resonance enhanced multiphoton ionization spectroscopy; rovibrational spectroscopic parameters for the $X\,^1\Sigma^+$ and $A\,^1\Pi$ states for the isotopomer ^{10}BH are also reported.
[c]Reference [7].
[d]Reference [8]. Emission spectroscopy; it is also given $H_e(a\,^3\Pi)=1.00\times 10^{-7}$ cm^{-1} and the spin-orbit constant $A(a\,^3\Pi)=4.388$ cm^{-1}.
[e]Reference [9].
[f]Reference [10]. FT spectroscopy.
[g]Reference [11]. Analysis of near UV spectroscopy.

as compared to an experimental value[7] of μ_0 $=1.27\pm 0.21$ D. For the $A\,^1\Pi$ state $\mu=0.591$ [Ref. [18(g)]] versus 0.58 ± 0.04 (Ref. [7]) D, while the calculated dipole moment of the $B\,^1\Sigma^+$ state is 4.677 D and pointing to the opposite direction as compared to the $X\,^1\Sigma^+$ and $A\,^1\Pi$ states.[18(g)]

The anion BH$^-$ was observed for the first time by Reid through double-charge-transfer mass spectrometry.[23] Except for the conclusion that "the equilibrium bond length in BH$^-$ is not too different from that of the uncharged BH molecule," no numerical results were reported.

Theoretically, the ground state ($X\,^2\Pi$) of the BH$^-$ species was studied for the first time by Griffing and Simons in 1975.[24] With the purpose to obtain the (adiabatic) electron affinity (EA) of BH, the authors estimated finally EA $=-0.22$ eV at the SCF/$[6s3p/_B\ 3s/_H]$ level. Three years later Rosmus and Meyer applied the coupled electron pair approximation (CEPA) method combined with a $[4s4p2d1f/_B\ 4s2p1d/_H]$ basis to the first and second row diatomic hydrides and their anions.[25] For the ground states they reported spectroscopic constants ($r_e,\omega_e,\omega_e x_e,a_e$) and EAs, the EA of BH being slightly positive, EA($X\,^2\Pi$) $=+0.03$ eV. This result was more or less confirmed eight years later via MP4/6-311++G($3df,3pd$) calculations, EA $=0.07$ eV,[26] whereas Pople et al.[27] obtained EA=0.12 eV at the MP4/6-31G** level. Relatively recently Morosi et al.[28] re-examined the EAs of the first row hydrides by Monte Carlo (MC) techniques. For the BH molecule they predicted 0.11 ± 0.01 and 0.81 ± 0.05 eV at the fixed-node diffusion

MC (FN-DMC) and variational MC approximations, respectively. They also obtained the dissociation energy of the BH$^-$ with respect to B(^2P)+H$^-$(^1S) fragments at the FN-DMC level, $D_e(X\,^2\Pi)=69.81\pm 0.26$ kcal/mol.[28]

On the B$_2$H$_2$ system the first publication appeared more than 30 years ago by Dill et al.,[29] who at the unrestricted Hartree–Fock level predicted a linear geometry (HBBH) with a ground state of $^3\Sigma_g^-$ symmetry and a $^1\Delta$ state 25 (UHF/STO-3G) or 34 (UHF/6-31G*) kcal/mol higher. Through CI+MP2/DZ+P calculations Jouany et al.[30] calculated the HB–BH dissociation energy with respect to the BH($X\,^1\Sigma^+$) fragments, $D_e=107$ kcal/mol. They also reported the location of the first two excited states, $^1\Delta_g$ and $^1\Sigma_g^+$, 16.6 and 26.3 kcal/mol higher. Next, Sana et al. obtained the harmonic frequencies of HBBH by the CISD/6-31G** method.[31] In 1993 Treboux and Barthelat investigated the $\widetilde{X}\,^3\Sigma_g^-$, $\widetilde{a}\,^1\Delta_g$, and $\widetilde{b}\,^1\Sigma_g^+$ group of states reporting equilibrium geometries as well as harmonic frequencies for the $\widetilde{X}\,^3\Sigma_g^-$ state at the CI+MP2/DZ+P level.[32] It is fair to say that these authors, for the first time, attributed the formation of the HBBH molecule to two BH($a\,^3\Pi$) moieties. With respect to two $a\,^3\Pi$ fragments they reported $D_e=153(\widetilde{X}\,^3\Sigma_g^-)$, $138(\widetilde{a}\,^1\Delta_g)$, and $130(\widetilde{b}\,^1\Sigma_g^+)$ kcal/mol.

Experimentally, the H^{10}B^{10}BH isotopomer was observed by Tague and Andrews, who ascribed an absorption band at 2679.9 cm^{-1} to the antisymmetric BH stretching mode through the help of MP2/TZ+P calculations.[33] The definitive experimental observation on HBBH, however, was ap-

peared one year later when Knight *et al.* confirmed its $\tilde{X}\,^3\Sigma_g^-$ symmetry by the electron spin resonance technique.[34]

A more systematic *ab initio* work on B_2H_2 was carried out by Perić *et al.*[35] who published MRDCI (Ref. 36) calculations using a $[5s3p1d/_B\,5s2p/_H]$ basis$+(2s1p1d)_B$ Rydberg-type functions located in the middle of the HB–BH distance ("bond functions"). Their first work[35(a)] deals with the construction of PECs of a series of electronic states with respect to the *cis* and *trans* bending modes, whereas the second one[35(b)] refers to full HB–BH PECs and PECs around the equilibrium of the HBB–H stretching. We will address to relative results of Ref. 35 later on.

Presently, we examine the molecules BH, BH⁻, and HBBH using high level multireference (complete active space self-consistent+single+double replacements $=$CASSCF+1+2$\equiv$MRCI) and coupled-cluster [mainly RCCSD(T)=restricted coupled-cluster+singles+doubles+perturbative connected triples[37]] methods, in conjunction with augmented quintuple-ζ quality basis sets. In particular, we have constructed 32 full PECs of BH which correlate adiabatically to the first eight states of B $[^2P(2s^22p^1),$ $^4P(2s^12p^2),$ $^2S^*(2s^23s^1),$ $^2D(2s^12p^2),$ $^2P^*(2s^23p^1),$ $^2D^*(2s^23d^1),$ $^2S^*(2s^24s^1),$ $^2P^*(2s^24p^1)]$ $+$H$[^2S(1s^1)]$ (Ref. 38), five of which (those marked by a *) are of Rydberg character. It is interesting that the $^2P^*(2s^23p^1)$ and $^2P^*(2s^24p^1)$ atomic states of B are missing from the Moore's tables,[39] while the ^4P is not accurately located yet.[38,39] For the BH⁻ we have obtained a definitive value of its ionization energy, and, for the first time, we report full PECs of the $X\,^2\Pi$ and $a\,^4\Sigma^-$ states at the same level of theory as in BH.

For the linear B_2H_2 system (HBBH), we have examined thoroughly its first three states, namely, $\tilde{X}\,^3\Sigma_g^-$, $\tilde{a}\,^1\Delta_g$, and $\tilde{b}\,^1\Sigma_g^+$.

The present work is structured as follows. In Sec. II we discuss the methods and computational details, in Sec. III we give results on the electronic structure of the B and B⁻ species, and in Sec. IV we discuss our findings on BH, BH⁻, and HBBH in the Secs. IV A–IV C, respectively. Section V epitomizes our work and highlights the central conclusions of this study.

II. METHODS

For the B atom the correlation consistent basis set with core functions of quintuple-ζ quality, cc-pCV5Z (=C5Z) was used through all our calculations.[40,41] Depending on the species studied, the C5Z basis was augmented by a double set of diffuse Gaussians (cc-pCV5Z+d-aug=dAC5Z) for the B, B⁻, and BH, by a single set of diffuse functions (AC5Z) for the BH⁻, whereas no augmentation was used for the HBBH molecule.[42] For the H atom the aug-cc-pV5Z (=A5Z) basis set was employed for BH and BH⁻ but the plain 5Z set for the HBBH system.[40] The doubly augmented basis set on B was deemed as necessary to describe the Rydberg molecular states of BH. These bases were generally contracted to $[9s8p7d6f5g3h/_B\,6s5p4d3f2g/_H]$=dAC5Z/A5Z for BH; $[8s7p6d5f4g2h/_B\,6s5p4d3f2g/_H]$=AC5Z/A5Z for BH⁻;

$[7s6p5d4f3g1h/_B\,5s4p3d2f1g/_H]$=C5Z/5Z for HBBH. The number of contracted spherical Gaussians are 268 (BH), 232 (BH⁻), and 342 (HBBH).

The internally contracted MRCI (=CASSCF+1+2) approach was applied as implemented in the MOLPRO2006.1 suite of codes.[43] The reference spaces (CASSCF) of BH were constructed by alloting the four active (valence) electrons to 18 orbitals: one 2s, three 2p, one 3s, three 3p, five 3d, one 4s, and three 4p on B, plus one 1s on H. Notice that the 3s, 3p, 3d, 4s, and 4p are Rydberg orbitals. The number of configuration functions (CFs) of the zeroth order space under C_{2v} symmetry constraints range from 2000 to 2400 (singlets), 2600 to 3000 (triplets), and about 800 (quintets). The CASSCF wave functions for the BH⁻ and HBBH systems were created by distributing five and eight valence electrons to five and ten molecular orbitals, respectively. These spaces range from about 20 (BH⁻) to 1600–2500 (HBBH) depending on the symmetry constraints. Dynamic ("hard") correlation was obtained by single and double excitations out of the reference spaces, always including the core electrons ($\sim 1s^2$) of the B atom. Internally contracted CI spaces range from 9×10^6 (singlets) to 14×10^6 (triplets) CFs in BH, about 3×10^5 for BH⁻, and around 17×10^6 CFs for HBBH. To cope with the large number of states (32) investigated in the BH system, we were forced to use the state averaged technique with the exception of the first three states, namely, $X\,^1\Sigma^+$, $a\,^3\Pi$, and $A\,^1\Pi$.

Single reference coupled-cluster calculations, RCCSD(T),[37] were also performed whenever possible and around equilibrium; in particular, for the BH molecule the states $X\,^1\Sigma^+$, $a\,^3\Pi$, $b\,^3\Sigma^-$, and $^5\Sigma^-$ were examined at the RCCSD(T) level. In addition, for certain properties of BH and BH⁻, the RCCSDT method as implemented in the MRCC code was applied as well.[44]

Spectroscopic parameters (ω_e, $\omega_e x_e$, a_e, and $\bar{D}_e$) for almost all states of BH examined and the two states of BH⁻ were obtained by solving the one dimensional rovibrational Schrödinger equation through a Numerov analysis. The basis set superposition error (BSSE) for BH in both the MRCI and RCCSD(T) methods at the dAC5Z/A5Z basis set level is negligible, i.e., 0.03 kcal/mol. The size nonextensivity error is small for the BH($X\,^1\Sigma^+$) and BH⁻($X\,^2\Pi$) and is getting significant, however, as we move to HBBH, 5(1) mE_h at the MRCI(+Q) level, where +Q refers to the Davidson correction.

III. THE B, B⁻, AND H⁻ SPECIES

Table II lists the energy separations ΔE_{0j} between the ground state and the first seven excited states ($j=1-7$) of the B atom, five of which are of Rydberg character, at the MRCI and CC level. The agreement between experiment and theory is very good at the MRCI+Q/dAC5Z level of theory, the largest discrepancy being 1247 cm^{-1} (2.3%) in the ΔE_{06} energy difference. It should be stressed at this point that single augmentation of the B basis set fails completely in predicting energy differences of Rydberg states, therefore double augmentation is mandatory.
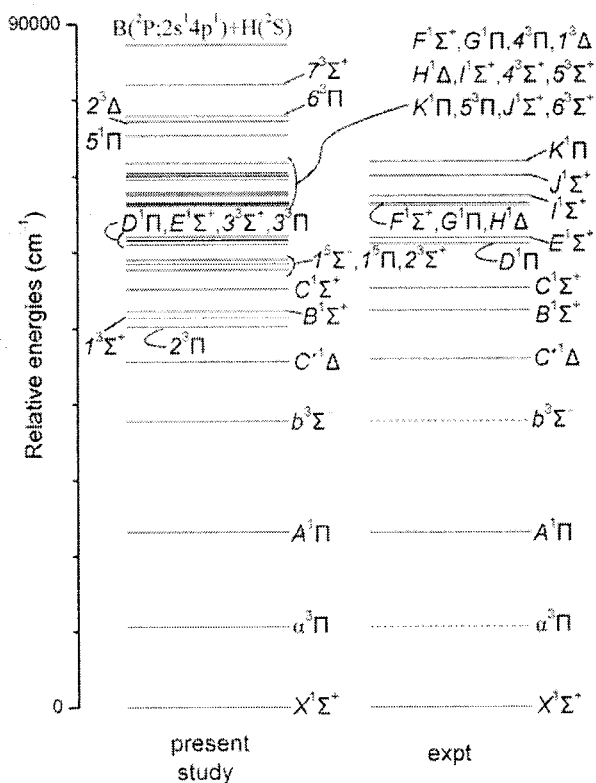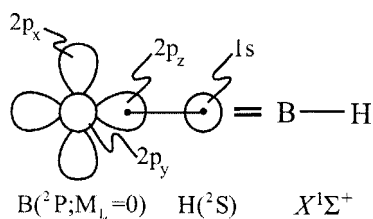
TABLE II. Calculated atomic energy separations (cm^{-1}) between the ground state of B(^2P; $2s^22p^1$) and its first seven excited states $^4P(2s^12p^2)$ (ΔE_{01}), $^2S^*(2s^23s^1)$ (ΔE_{02}), $^2D(2s^12p^2)$ (ΔE_{03}), $^2P^*(2s^23p^1)$ (ΔE_{04}), $^2D^*(2s^23d^1)$ (ΔE_{05}), $^2S^*(2s^24s^1)$ (ΔE_{06}), $^2P^*(2s^24p^1)$ (ΔE_{07}), and B$^-$(^3P; $2s^22p^2$) $\rightarrow$B$^-$(^5S; $2s^12p^3$) (ΔE^-). The $*$ symbol signifies Rydberg states.

Method[a]	ΔE_{01}	ΔE_{02}	ΔE_{03}	ΔE_{04}	ΔE_{05}	ΔE_{06}	ΔE_{07}	ΔE^-
MRCI	28 878	39 999	48 178	48 604	54 900	55 896	57 765	22 502
MRCI+Q	28 884	40 000	47 949	48 585	55 209	56 247	58 008	22 824
RCCSD(T)	28 793	39 956		48 518		56 021	57 709	22 105
RCCSDT	28 880	40 043		48 628				22 402
Expt.[b]	28 867.15	40 029.48	47 846.95	48 602.84	54 757.57	55 000.01	57 776.63	22 477[b,c]

[a]Basis set dAC5Z; +Q refers to the Davidson correction.
[b]References 38 and 39 (M_J averaged).
[c]References 45 and 46; see text.

The experimental EA of the B atom is EA=E(B; ^2P) $-E$(B$^-$; ^3P)=0.2797 eV,[45] as contrasted to 0.09 (0.24) and 0.25 (0.27) eV at the MRCI(+Q) and RCCSD(T) (RCCSDT)/dAC5Z levels of theory, respectively. It is remarkable that the MRCI/dAC5Z fails to produce a reasonable EA of the B atom, obviously due to size nonextensivity errors. It is interesting that at the valence MRCI/dAC5Z level [correlating 3(B) and 4(B$^-$) electrons], EA =0.13(0.26) eV.

The first two excited states of B$^-$(^3P) are expected to be ^1D and ^1S; of interest to the present work is also the ^5S of B$^-$. Experimentally, the ^1D of B$^-$ is unbound with respect to the ^2P state of B by 0.104 eV,[47] located 0.3837 eV (=3095 cm^{-1}) above the B$^-$ ^3P state.[45] No experimental results seem to exist for the ^1S state of B$^-$, whereas a "semiexperimental" estimate of the B$^-$ ^3P-^5S splitting can be obtained from the relation, ΔE[B$^-$(^3P)$\rightarrow$B$^-$(^5S)] = ΔE[B$^-$(^3P) $\rightarrow$ B(^2P)] + ΔE[B(^2P)$\rightarrow$B(^4P)]$-\Delta E$[B$^-$(^5S) $\rightarrow$B(^4P)]=2256.12(Ref. 45) +28867.15 (Ref. 38) −8646.3 (Ref. 46) =22477 cm^{-1}. Note that the B$^-$(^5S)−B(^4P) splitting is the result of a theoretical finite element multiconfigurational Hartree–Fock calculation by Froese et al.[46] Of course, the ^1S and ^5S states of B$^-$ are unbound with respect to the ^2P state of neutral B. Our MRCI+Q/dAC5Z for the B$^-$ ^3P-^1D, ^3P-^1S, and ^3P-^5S splittings are 2954, 6233, and 22 824 cm^{-1}, respectively; see Table II.

Finally, the experimental EA of the H atom, E(H; ^2S) $-E$(H$^-$; ^1S), is 0.7542 eV,[48] as compared to the CISD/dA5Z (A5Z) value of 0.7517 (0.7465) eV obtained presently.

IV. RESULTS AND DISCUSSION

A. BH

For all the 32 states being derived from the channels {B(^2P; $2s^22p^1$), B(^4P; $2s^12p^2$), B($^2S^*$; $2s^23s^1$), B(^2D; $2s^12p^2$), B($^2P^*$; $2s^23p^1$), B($^2D^*$; $2s^23d^1$), B($^2S^*$; $2s^24s^1$), B($^2P^*$; $2s^24p^1$)}+H(^2S), namely, {($^{1,3}\Sigma^+$, $^{1,3}\Pi$); ($^{3,5}\Sigma^-$, $^{3,5}\Pi$); $^{1,3}\Sigma^+$; ($^{1,3}\Sigma^+$, $^{1,3}\Pi$, $^{1,3}\Delta$); ($^{1,3}\Sigma^+$, $^{1,3}\Pi$); ($^{1,3}\Sigma^+$, $^{1,3}\Pi$, $^{1,3}\Delta$); $^{1,3}\Sigma^+$; ($^{1,3}\Sigma^+$, $^{1,3}\Pi$)}, complete PECs have been constructed at the MRCI/dAC5Z level of theory; see Figs. 1 and 2. With the exception of the 1 $^5\Pi$ and 1 $^3\Sigma^+$ states which are of repulsive nature, 30 states are bound with binding energies ranging from about 2.5 ($^5\Sigma^-$) to 90 kcal/mol (C' $^1\Delta$). Table III collects all our results including experimental findings for comparison. States tagged with

a Latin capital or lower-case letter have been observed experimentally; all but the a $^3\Pi$ and b $^3\Sigma^-$ states are singlets. The rest are labeled by a number in front of the molecular term symbol, indicating states of the same symmetry in ascending energy order.

We first discuss the eight states correlating adiabatically to the first two channels and then the three states C' $^1\Delta$,B $^1\Sigma^+$, and C $^1\Sigma^+$, covering at the same time the seven experimentally characterized states.

1. $X\,^1\Sigma^+$, $a\,^3\Pi$, $A\,^1\Pi$, $1\,^3\Sigma^+$

Figure 1 shows the PECs of these states correlating to the ground state atoms B(^2P)+H(^2S). The X $^1\Sigma^+$ state can be clearly described by the following valence-bond-Lewis (vbL) diagram; see also Table IV.

FIG. 1. Potential energy curves of the first 32 electronic states of the BH molecule at the MRCI/dAC5Z level of theory.

FIG. 2. Calculated vs experimentally measured energy separations of several states of BH. Since $T_e(a\,^3\Pi)$ is experimentally unknown, the corresponding level has been set to our calculated value, while the experimental $b\,^3\Sigma^-$ line has been drawn 27 152.8 cm^{-1} (=experimental $a\,^3\Pi$-$b\,^3\Sigma^-$ separation) higher.


By coupling the active electrons into a triplet, the $1\,^3\Sigma^+$ state is obtained which is of repulsive character, with a van der Waals interaction of about 7 cm^{-1} at 9.3 a.u. An avoided crossing at 2.32 a.u. with another $^3\Sigma^+$ state correlating to B($^2S^*$; $2s^23s^1$) creates a shoulder to the PEC of the $1\,^3\Sigma^+$ state at an energy distance of about 51 500 cm^{-1} from the X-state.

The experimental binding energy of the $X\,^1\Sigma^+$ state is $D_0=82.5\pm0.43$ kcal/mol;[11] this value has been finally corrected to $D_0=81.6\pm0.6$ kcal/mol (*vide supra*).[12] Our MRCI [or RCCSD(T)] value is $D_e=84.78$ kcal/mol with the zero point energy (ZPE)=3.34 kcal/mol, calculated by solving the one dimensional rovibrational Schrödinger equation; thus $D_0=81.44$ kcal/mol. Including scalar relativistic effects obtained by the second order Douglas–Kroll–Hess[49] approximation (+0.02 kcal/mol) and the BSSE correction (−0.03 kcal/mol), we finally obtain $D_0=81.43$ kcal/mol, in excellent agreement with the "experimental" value, as suggested in Ref. 12. This D_0 value is also in complete agreement with the CCSD(T)/CBS result of Feller *et al.*,[15]

$D_0=81.6$ kcal/mol. As can be seen from Table III, the spectroscopic parameters ω_e, $\omega_e x_e$, a_e, and $\bar{D}_e$ are in very good agreement with the corresponding experimental numbers. Our MRCI [or RCCSD(T)] dipole moment μ determined by the finite field method, $\mu_e^{(FF)}=1.403$ D, is in complete agreement with the "estimated" full-CI result of Halkier *et al.*,[22] $\mu_e=1.398\pm0.004$ D. This is a definitive dipole moment value of the $X\,^1\Sigma^+$ state of BH and should be contrasted with the experimental value, $\mu_0=1.27\pm0.21$ D.[7]

The first excited state of BH is of $^3\Pi$ symmetry and as was already mentioned it correlates adiabatically to B(^2P)+H(^2S), however, *diabatically* it correlates to the first excited state of B(^4P) due to its strong interaction with the $2\,^3\Pi$ state; the latter correlates *adiabatically* to B(^4P)+H(^2S). For this reason the vbL diagram looks as follows:
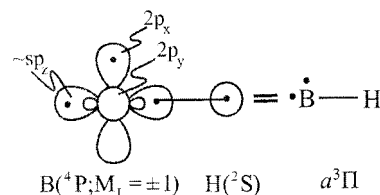
The picture above is strongly supported by the atomic Mulliken populations (Table IV). Because of the "opening" of the $2s^2$ distribution of B, one expects a shorter bond length, a larger ω_e, and a higher (diabatic) dissociation energy as compared to the $X\,^1\Sigma^+$ state. This is exactly what is happening: The r_e is shorter by 0.04 Å, the ω_e larger by 250 cm^{-1}, and the internal bond strength higher by 52.3 kcal/mol. As a matter of fact, the $a\,^3\Pi$ state has the shorter bond length and the highest *diabatic* D_e of all states studied. From Table III we can see that all our calculated values are in excellent agreement with the experimental results. The experimental bond distance, $r_0=1.2006$ Å,[9] should be compared to our $r_0=1.2021$ (1.2013) Å at the MRCI [RCCSD(T)] level. Finally, note that the $X\,^1\Sigma^+$-$a\,^3\Pi$ splitting is experimentally unknown, but our MRCI [RCCSD(T)] value of 10 588 (10 581) cm^{-1} should be very reliable. A comment for the dipole moment is necessary: Experimentally the dipole moment of the $a\,^3\Pi$ state has not been determined, and as far as we know this is the first time that it has been calculated, $\mu=0.22$ D. It is more than six times smaller than that of $X\,^1\Sigma^+$ state, the reason being the one electron σ (sp_z) distribution on the back of the B atom as is indicated in the vbL diagram of the $a\,^3\Pi$ state.

The PEC of the $A\,^1\Pi$ open singlet state presents an interesting hump with its maximum located at 2.11 Å and a height of 2.01 (1.95) kcal/mol at the MRCI(+Q)/dAC5Z level; see Fig. 1. The same value is obtained by the workers of Refs. 12 and 19, namely, 1.9 ± 0.2 and $1.95-2.00$ kcal/mol, respectively. The bonding vbL diagram, in accordance with the Mulliken atomic distributions of Table IV, is as follows.
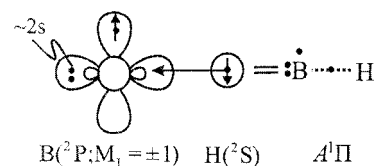
TABLE III. Total energies E (E_h), equilibrium bond distances r_e (Å), dissociation energies D_e (kcal/mol), harmonic and anharmonic frequencies ω_e, $\omega_e x_e$ (cm^{-1}), rotational-vibrational coupling constants a_e (cm^{-1}), centrifugal distortions $\bar{D}_e$ (cm^{-1}), dipole moments μ (D), and energy separations T_e (cm^{-1}) of 32 electronic states of the ^{11}B^{1}H molecule. Basis set dAC5Z/$_B$ A5Z/$_H$.

Method	$-E$	r_e	D_e[a]	ω_e	$\omega_e x_e$	a_e	$\bar{D}_e$	$\mu_{FF}(\langle\mu\rangle)$[b]	T_e
				$X\ ^1\Sigma^+$					
MRCI	25.287 578	1.230 1	84.78	2358	48.5	0.419	1.23	1.403(1.405)	0.0
MRCI+Q	25.287 78	1.230	84.8	2359	48.8	0.418	1.23	1.403	0.0
RCCSD(T)	25.257 203	1.229 6	84.78	2361	49.0	0.417	1.24	1.408	0.0
RCCSDT	25.287 650	1.230 4	84.78					1.403	0.0
Expt[c]		1.232 18	82.5[d] ±0.4	2366.7	49.3	0.422	1.23	1.27±0.21	0.0
				2364.7	47.7	0.422	1.23		0.0
				$a\ ^3\Pi$					
MRCI	25.239 335	1.189 7	54.51	2625	60.4	0.455	1.23	0.22(0.22)	10 588
MRCI+Q	25.239 56	1.190	54.6	2625	60.4	0.455	1.22	0.22	10 583
RCCSD(T)	25.238 994	1.187 7	54.33	2631	54.0	0.416	1.23	0.22	10 581
Expt[c]		1.200 6[e]		2625.1	55.8	0.416	1.23		x
				$A\ ^1\Pi$					
MRCI	25.181 986	1.221 9	18.51	2340	130.0	0.853	1.68	0.56(0.56)	23 175
MRCI+Q	25.182 33	1.222	18.7	2341	129.6	0.851	1.67	0.56	23 144
Expt[c]		1.218 6		2251.5	56.6	0.835	1.46	0.58±0.04	23 105.1
				2342.4	127.8	0.538			
				$b\ ^3\Sigma^-$					
MRCI	25.115 655	1.217 3	59.51	2436	59.3	0.452	1.23	−0.44(−0.44)	37 733[f]
MRCI+Q	25.115 97	1.217	59.6	2430	57.3	0.459	1.22	−0.44	37 708[f]
RCCSD(T)	25.114 675	1.215 5	58.82	2440	55.9	0.442	1.04	−0.45	37 866[f]
Expt[c]		1.227 1[g]		2438.1	55.6	0.431	1.26		x+27 152.8
				$C'\ ^1\Delta$					
MRCI	25.073 041	1.198 1	89.58	2578	44.0	0.379	1.15	−0.58(−0.58)	47 085
MRCI+Q	25.079 92	1.197	89.7	2618	48.0	0.384	1.14	−0.57	45 620
Expt[c]		1.196 3		2610.0	46.6	0.390	1.22		45 981.0
				$2\ ^3\Pi$					
MRCI	25.057 216	1.937 1	23.24	1309	42.4	0.104	0.38	−0.06(−0.09)	50 559
MRCI+Q	25.058 98	1.931	23.8	1295	38.6	0.099	0.39	−0.06	50 216
				$1\ ^3\Sigma^+$					
MRCI	25.052 075	1.23							51 688
				$B\ ^1\Sigma^+$					
MRCI	25.048 126	1.214 9[h]	49.63	2416	84.4	0.591	1.36	−3.41(−3.33)	52 554
MRCI+Q	25.049 60	1.214[h]	49.6	2237	⋯	0.575	1.33	−3.23	52 274
Expt[c]		1.216 4		2399.9	69.5	0.485	1.26		52 335.8
				$C\ ^1\Sigma^+$					
MRCI	25.031 701	1.213 2	63.72	2442	49.9	0.428	1.19	−1.22(−1.15)	56 159
MRCI+Q	25.036 21	1.214	62.3	2463	53.1	0.431	1.20	−1.51	55 213
Expt[c]		1.212 9		2474.7	54.4	0.432	1.25		55 281.1
				$1\ ^5\Sigma^-$					
MRCI	25.024 825	1.702 2	2.47	525	87.6	1.571	6.05	1.47(1.47)	57 668
MRCI+Q	25.025 00	1.701	2.50	528	87.3	1.532	5.23	1.47	57 674
RCCSD(T)	25.024 805	1.697 0	2.41	502	78.5	1.394	4.56	1.47	57 590

TABLE III. (*Continued.*)

Method	$-E$	r_e	D_e[a]	ω_e	$\omega_e x_e$	a_e	$\bar{D}_e$	$\mu_{FF}(\langle\mu\rangle)$[b]	T_e
				$1\ ^5\Pi$[i]					
MRCI	25.020 926	4.85	0.02						58 523
MRCI+Q	25.021 05	4.82	0.02						58 540
				$2\ ^3\Sigma^+$					
MRCI	25.017 837	1.216 9	30.11	1462($=\Delta G_{1/2}$)				1.86(1.90)	59 201
MRCI+Q	25.018 97	1.223	31.8	1510($=\Delta G_{1/2}$)				1.75	58 997
				$D\ ^1\Pi$					
MRCI	25.006 572	1.200 7	47.89	2642	159.1	0.939	1.82	0.41(0.45)	61 674
MRCI+Q	25.009 72	1.202	45.6	2660	172.0	1.032	2.02	0.35	61 027
Expt[c]		1.217 3[j]					1.3		61 105.4
				$E\ ^1\Sigma^+$					
MRCI	25.003 314	1.197 3	46.72	2587	78.7	0.541	1.30	817(7.92)	62 389
MRCI+Q	25.006 94	1.198	47.6	2589	75.4	0.528	1.29	7.42	61 637
Expt[c]									61 872.3
				$3\ ^3\Sigma^+$					
MRCI	25.004 289	1.322 7	46.22	2404	69.1	0.277	1.21	380(3.84)	62 174
MRCI+Q	25.007 46	1.304	45.4	2634	108.7	0.346	1.19	3.69	61 523
				$3\ ^3\Pi$					
MRCI	25.001 840	1.323 7	44.28	2606($=\Delta G_{1/2}$)					62 712
MRCI+Q	25.004 80	1.316	43.9	2678($=\Delta G_{1/2}$)					62 107
				$F\ ^1\Sigma^+$					
MRCI	24.985 329	1.220 2	53.12	2387	92.5	0.647	1.42	0.14(0.18)	66 336
MRCI+Q	24.986 65	1.221	53.2	2341	87.8	0.643	1.41	0.30	66 090
Expt[c]									66 079.5
				$G\ ^1\Pi$					
MRCI	24.983 898	1.208 9	34.35	2191($=\Delta G_{1/2}$)				0.48(0.41)	66 650
MRCI+Q	24.985 34	1.209	33.9	2160($=\Delta G_{1/2}$)				0.60	66 378
Expt[c]		1.220 6[k]							66 399.3
				$4\ ^3\Pi$					
MRCI	24.981 704	1.262 1	33.24	2643($=\Delta G_{1/2}$)					67 132
MRCI+Q	24.984 62	1.246	33.5	2651($=\Delta G_{1/2}$)					66 536
				$1\ ^3\Delta$					
MRCI	24.985 032	1.202 7	34.22	2547	86.2	0.611	1.41	0.45(0.45)	66 401
MRCI+Q	24.985 88	1.202	30.7	2584	95.7	0.643	1.47	0.46	66 259
				$H\ ^1\Delta$					
MRCI	24.983 458	1.202 0	51.91	2549	72.1	0.518	1.27	0.41(0.42)	66 747
MRCI+Q	24.984 82	1.202	52.1	2549	71.6	0.515	1.27	0.42	66 492
Expt[c]									66 419.7
				$1\ ^1\Sigma^+$					
MRCI	24.976 152	1.205 6	50.10	2516	79.6	0.558	1.33	−14.6(−13.3)	68 350
MRCI+Q	24.978 74	1.206	51.2	2505	76.9	0.551	1.31	−13.3	67 826
Expt[c]		1.23 4[l]							67 395.8
				$4\ ^3\Sigma^+$					
MRCI	24.979 176	1.204 1	34.30	2449	60.4	0.513	1.33	−8.65(−8.58)	67 686
MRCI+Q	24.980 01	1.204	33.2	2527	81.8	0.594	1.43	−8.68	67 548

TABLE III.   (*Continued.*)

Method	$-E$	r_e	D_e[a]	ω_e	$\omega_e x_e$	a_e	$\bar{D}_e$	$\mu_{FF}(\langle\mu\rangle)$[b]	T_e
				$5\,^3\Sigma^+$					
MRCI	24.970 271	1.201 2	45.60	2519	70.4	0.539	1.32	7.23(7.45)	69 641
MRCI+Q	24.971 02	1.200	45.4	2561	81.7	0.577	1.36	7.23	69 521
				$K\,^1\Pi$					
MRCI	24.966 751	1.199 2	41.32	2174(=$\Delta G_{1/2}$)				1.38(0.57)	70 413
MRCI+Q	24.969 04	1.202	42.1	2100(=$\Delta G_{1/2}$)				0.93	69 955
Expt[c]									71 840
				$5\,^3\Pi$					
MRCI	24.967 039	1.195 7	41.62	3125	168.9	0.861	0.88		70 350
MRCI+Q	24.968 53	1.164	41.5	2901	119.2	0.862	0.90		70 067
				$J\,^1\Sigma^+$					
MRCI	24.964 313	1.200 7	48.01	2586	77.2	0.528	1.28	12.9(11.3)	70 948
MRCI+Q	24.967 03	1.202	48.9	2548	71.3	0.516	1.27	12.2	70 396
Expt[c]									70 040
				$6\,^3\Sigma^+$					
MRCI	24.956 453	1.311 4	40.63	1900(=$\Delta G_{1/2}$)				1.65(0.70)	72 674
MRCI+Q	24.961 33	1.272	42.8	2202(=$\Delta G_{1/2}$)				2.18	71 647
				$5\,^1\Pi$					
MRCI	24.936 149	1.461 9	30.17	1968(=$\Delta G_{1/2}$)					77 130
MRCI+Q	24.944 54	1.472	34.7	2372(=$\Delta G_{1/2}$)					75 332
				$2\,^3\Delta$					
MRCI	24.928 196	1.584 8	17.06	1399(=$\Delta G_{1/2}$)				1.23(1.13)	78 875
MRCI+Q	24.936 49	1.550	21.6	1523(=$\Delta G_{1/2}$)				1.32	77 099
				$6\,^3\Pi$					
MRCI	24.930 922	1.281 8	27.20	1918	112.4	0.915	1.78	−1.92(−1.77)	78 277
MRCI+Q	34.933 04	1.287	27.6	1700(=$\Delta G_{1/2}$)				−2.01	77 812
				$7\,^3\Sigma^+$					
MRCI	24.910 267	1.90	13.5						82 810
MRCI+Q	24.914 60	1.87	15.3						81 904

[a]With respect to the adiabatic fragments.

[b]Finite field method (μ_{FF}), expectation value ($\langle\mu\rangle$). Field intensity=10^{-5} a.u. The positive direction of the dipole moment vector is defined as B$^-$−H$^+$.

[c]See Table I.

[d]D_0 from Ref. 11, but see text.

[e]r_0. Our calculated MRCI (MRCI+Q) [RCCSD(T)] r_0 is 1.2021(1.202) [1.2013] Å.

[f]Since the experimental $a\,^3\Pi$-$b\,^3\Sigma^-$ energy separation is known (=27 152.8 cm^{-1}), we also report our calculated $a\,^3\Pi$-$b\,^3\Sigma^-$ separation at MRCI (MRCI+Q) [RCCSD(T)]: 27 145 (27 125) [27 285] cm^{-1}.

[g]r_0. Our calculated MRCI (MRCI+Q) [RCCSD(T)] r_0 is 1.2311 (1.231) [1.2294] Å.

[h]A second (ionic) minimum is found at 3.023 (3.019) Å at the MRCI (+Q) level lying 6097 (5540) cm^{-1} above the first one; see Fig. 1.

[i]The 1 $^3\Pi$ state is of repulsive character; the 0.02 kcal/mol ($\approx$7 cm^{-1}) is clearly a van der Waals interaction.

[j]r_0. Our calculated MRCI (MRCI+Q) r_0 is 1.2157 (1.217) Å.

[k]r_0. Our calculated MRCI (MRCI+Q) r_0 is 1.2246 (1.225) Å.

[l]r_0. Our calculated MRCI (MRCI+Q) r_0 is 1.2193 (1.220) Å.

A half σ bond is formed by a transfer of $0.12e^-$ from the H atom to the empty $2p_z$ orbital of the B atom. As the H atom moves from infinity toward equilibrium, interacts repulsively with the ~$2s^2$ distribution of B, hence the barrier, then the attractive interaction takes over pushing synchronously the hybridized by now $(2s2p_z)^2$ distribution on the back of the B atom. A much lower binding energy is expected; indeed D_e=18.5 kcal/mol or D_0=15.25 kcal/mol. The rest of our calculated values can be considered in very good agreement with the experimental values including the dipole moment (Table III).

2. $b\,^3\Sigma^-$, 2 $^3\Pi$, 1 $^5\Sigma^-$, 1 $^5\Pi$

These states correlate to the channel B(^4P; $2s^1 2p^2$) +H(^2S); the $b\,^3\Sigma^-$ and 2 $^3\Pi$ are well bound, the 1 $^5\Sigma^-$ is

TABLE IV. Dominant equilibrium MRCI configurations, corresponding Mulliken atomic populations, and total charge on the boron atom of the BH molecule for 29 bound states.

State	Dominant equilibrium CASSCF configurations	Populations B									H	
		s	p_z	p_x	p_y	$3d_{z^2}$	$3d_{xz}$	$3d_{yz}$	$3d_{x^2-y^2}$	$3d_{xy}$	$1s$	q_B
$X\,^1\Sigma^+$	$0.96\lvert2\sigma^23\sigma^2\rangle-0.19\lvert2\sigma^2(1\pi_x^2+1\pi_y^2)\rangle$	1.69	1.05	0.06	0.06	0.04	0.01	0.01	0.00	0.00	1.04	+0.07
$a\,^3\Pi$	$0.98\lvert2\sigma^23\sigma^11\pi_x^1\rangle$	1.27	0.72	0.98	0.02	0.01	0.00	0.00	0.00	0.00	0.93	−0.02
$A\,^1\Pi$	$0.98\lvert2\sigma^23\sigma^1\overline{1\pi_x^1}\rangle+0.14\lvert2\sigma^13\sigma^14\sigma^1\overline{1\pi_x^1}\rangle$	1.48	0.60	0.97	0.03	0.01	0.00	0.00	0.00	0.00	0.85	−0.12
$b\,^3\Sigma^-$	$0.95\lvert2\sigma^21\pi_x^11\pi_y^1\rangle-0.19\lvert2\sigma^13\sigma^1(\overline{1\pi_x^1}1\pi_y^1+1\pi_x^1\overline{1\pi_y^1})\rangle$	1.04	0.13	0.98	0.98	0.01	0.00	0.00	0.00	0.00	0.79	−0.16
$C'\,^1\Delta$	$0.67\lvert2\sigma^23\sigma^2(1\pi_x^2-1\pi_y^2)\rangle$	1.05	0.13	0.95	0.95	0.01	0.01	0.01	0.00	0.00	0.78	−0.07
$2\,^3\Pi$	$0.78\lvert2\sigma^13\sigma^21\pi_x^1\rangle+0.52\lvert2\sigma^24\sigma^11\pi_x^1\rangle-0.22\lvert2\sigma^14\sigma^21\pi_x^1\rangle$	1.18	0.75	0.99	0.02	0.01	0.00	0.00	0.00	0.00	1.01	+0.02
$B\,^1\Sigma^+$	$0.93\lvert2\sigma^23\sigma^1\overline{4\sigma^1}\rangle-0.15\lvert2\sigma^23\sigma^2(1\pi_x^2+1\pi_y^2)\rangle$	2.13	0.76	0.08	0.08	0.02	0.00	0.00	0.00	0.00	0.84	−0.14
$C\,^1\Sigma^+$	$0.62\lvert2\sigma^23\sigma^2(1\pi_x^2+1\pi_y^2)\rangle+0.22\lvert2\sigma^23\sigma^1\overline{4\sigma^1}\rangle$	1.14	0.33	0.84	0.84	0.01	0.01	0.01	0.01	0.01	0.69	−0.20
$1\,^5\Sigma^-$	$0.99\lvert2\sigma^13\sigma^11\pi_x^11\pi_y^1\rangle$	0.99	0.22	0.98	0.98	0.02	0.00	0.00	0.00	0.00	0.75	−0.21
$2\,^3\Sigma^+$	$\lvert2\sigma^23\sigma^1[0.61(6\sigma^1)+0.50(5\sigma^1)+0.40(4\sigma^1)]\rangle$	1.45	1.68	0.02	0.02	0.06	0.00	0.00	0.00	0.00	0.54	−0.25
$D\,^1\Pi$	$0.92\lvert2\sigma^23\sigma^1\overline{2\pi_x^1}\rangle+0.20\lvert2\sigma^23\sigma^1\overline{4\pi_x^1}\rangle$	1.41	0.76	1.04	0.02	0.02	0.01	0.00	0.00	0.00	0.71	−0.27
$E\,^1\Sigma^+$	$0.75\lvert2\sigma^23\sigma^1\overline{5\sigma^1}\rangle-0.48\lvert2\sigma^23\sigma^1\overline{9\sigma^1}\rangle$	1.60	1.49	0.07	0.07	0.01	0.00	0.00	0.00	0.00	0.65	−0.26
$3\,^3\Sigma^+$	$\lvert2\sigma^23\sigma^1[0.63(6\sigma^1)-0.56(4\sigma^1)-0.36(5\sigma^1)]\rangle$	1.52	1.06	0.05	0.05	0.49	0.00	0.00	0.00	0.00	0.74	−0.18
$3\,^3\Pi$	$0.95\lvert2\sigma^23\sigma^12\pi_x^1\rangle$	1.39	0.80	1.03	0.02	0.01	0.00	0.00	0.00	0.00	0.69	−0.29
$F\,^1\Sigma^+$	$0.67\lvert2\sigma^23\sigma^1\overline{7\sigma^1}\rangle-0.62\lvert2\sigma^23\sigma^1\overline{6\sigma^1}\rangle$	1.49	0.84	0.00	0.00	0.78	0.00	0.00	0.00	0.00	0.76	−0.18
$G\,^1\Pi$	$0.96\lvert2\sigma^23\sigma^1\overline{3\pi_x^1}\rangle$	1.43	0.77	0.04	0.02	0.02	0.95	0.00	0.00	0.00	0.68	−0.24
$4\,^3\Pi$	$0.89\lvert2\sigma^23\sigma^13\pi_x^1\rangle+0.30\lvert2\sigma^23\sigma^14\pi_x^1\rangle$	1.47	0.72	0.08	0.03	0.01	0.93	0.00	0.00	0.00	0.67	−0.26
$1\,^3\Delta$	$0.97\lvert2\sigma^23\sigma^11\delta^1\rangle$	1.40	0.78	0.03	0.03	0.02	0.00	0.00	0.99	0.00	0.69	−0.02
$H\,^1\Delta$	$0.97\lvert2\sigma^23\sigma^1\overline{1\delta^1}\rangle$	1.43	0.75	0.03	0.03	0.02	0.00	0.00	0.98	0.00	0.69	−0.26
$I\,^1\Sigma^+$	$0.70\lvert2\sigma^23\sigma^1\overline{5\sigma^1}\rangle-0.62\lvert2\sigma^23\sigma^1\overline{6\sigma^1}\rangle$	1.95	0.88	0.03	0.03	0.13	0.00	0.00	0.00	0.00	0.93	−0.03
$4\,^3\Sigma^+$	$\lvert2\sigma^23\sigma^1[0.84(8\sigma^1)+0.32(5\sigma^1)]\rangle$	1.92	0.80	0.02	0.02	0.18	0.00	0.00	0.00	0.00	1.00	−0.26
$5\,^3\Sigma^+$	$\lvert2\sigma^23\sigma^1[0.87(7\sigma^1)+0.27(6\sigma^1)]\rangle$	1.31	1.94	0.02	0.02	0.01	0.00	0.00	0.00	0.00	0.57	+0.05
$K\,^1\Pi$	$0.93\lvert2\sigma^23\sigma^1\overline{4\pi_x^1}\rangle-0.15\lvert2\sigma^23\sigma^1\overline{2\pi_x^1}\rangle$	1.41	0.77	1.07	0.02	0.02	0.01	0.00	0.00	0.00	0.70	−0.30
$5\,^3\Pi$	$0.95\lvert2\sigma^23\sigma^14\pi_x^1\rangle$	1.42	0.76	1.07	0.02	0.02	0.02	0.00	0.00	0.00	0.76	−0.32
$J\,^1\Sigma^+$	$0.83\lvert2\sigma^23\sigma^19\sigma^1\rangle+0.45\lvert2\sigma^23\sigma^1\overline{5\sigma^1}\rangle$	1.38	1.89	0.03	0.03	0.03	0.00	0.00	0.00	0.00	0.51	−0.37
$6\,^3\Sigma^+$	$\lvert2\sigma^23\sigma^1[0.88(9\sigma^1)+0.18(6\sigma^1)]\rangle$	1.17	0.65	0.07	0.07	0.99	0.00	0.00	0.00	0.00	0.80	−0.31
$5\,^1\Pi$	$0.92\lvert2\sigma^24\sigma^1\overline{1\pi_x^1}\rangle$	2.04	0.25	0.97	0.02	0.03	0.01	0.00	0.00	0.00	0.57	−0.33
$2\,^3\Delta$	$0.67\lvert2\sigma^23\sigma^14\sigma^1(1\pi_x^2-1\pi_y^2)\rangle$	1.02	0.35	0.87	0.87	0.02	0.02	0.02	0.09	0.09	0.65	−0.27
$6\,^3\Pi$	$0.94\lvert2\sigma^24\sigma^11\pi_x^1\rangle$	2.03	0.17	0.97	0.02	0.00	0.00	0.00	0.00	0.00	0.67	−0.24

weakly bound by 2.5 kcal/mol, whereas the 1 $^5\Pi$ is purely repulsive as expected with a van der Waals interaction of about 7 cm^{-1} at 9.20 a.u.; Fig. 1. The vbL diagram of the $b\,^3\Sigma^-$ state is shown below.

$$B(^4P; M_L=0)\quad H(^2S)\qquad b^3\Sigma^-$$
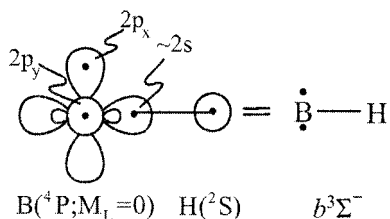
Clearly the σ bond is formed by a transfer of about $0.2e^-$ from the H atom to a $2s2p_z$ hybrid on B. The bonding MRCI orbital is $2\sigma\approx(0.76)\cdot2s^B+(0.28)\cdot2p_z{}^B+(0.72)\cdot1s^H$ (Table IV). At the MRCI [RCCSD(T)]/dAC5Z level the r_e and r_0 values are 1.2173 [1.2155] and 1.2311 [1.2294] Å, respectively, longer by 0.004 [0.0023] Å from experiment.[9] The adiabatic MRCI binding energy is $D_e=59.5$ kcal/mol, and the $a\,^3\Pi$-$b\,^3\Sigma^-$ energy difference 27 145 cm^{-1} in complete agreement with the experimental value[8] of 27 153 cm^{-1}.

The 2 $^3\Pi$ is a state of multireference character interacting strongly (*vide supra*) with the $a\,^3\Pi$, thus with a complicated bonding (see Table IV). It has the longest bond length

of all states studied ($r_e=1.93-1.94$ Å) with a dipole moment close to zero, and a $T_e(X\,^1\Sigma^+$-$2\,^3\Pi)\approx50\,500$ cm^{-1}. No experimental data exist and although it can be considered as well bound ($D_e=23-24$ kcal/mol), the prospects of being observed experimentally are dim due to spin and Franck–Condon factors (Fig. 1).

The $^5\Sigma^-$ state is obtained from $b\,^3\Sigma^-$ but with the four electrons coupled into a quintet (see previous vbL diagram). At short internuclear distance the Pauli forces polarize the $2p_z$ B electron to the back, resulting to a very weak bond of 2.5 kcal/mol at $r_e\approx1.70$ Å, with a concomitant electron transfer from H to the $2p_z$ orbital of B of about $0.25e^-$; see Fig. 1 and Tables III and IV.

3. $C'\,^1\Delta$, $B\,^1\Sigma^+$, $C\,^1\Sigma^+$

The $C'\,^1\Delta$ and $C\,^1\Sigma^+$ states dissociate adiabatically to B(^2D; $2s^12p^2$)+H(^2S), located experimentally 45 981.0 and 55 281.1 cm^{-1} above the X-state.[9] Our theoretical MRCI+Q values are 45 620 and 55 213 cm^{-1}, respectively; Table III. Their vbL diagrams indicating their bonding character are the following:
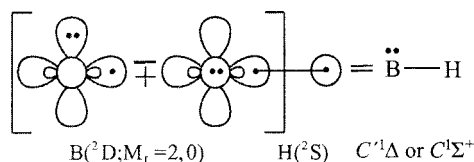
The "$-$" sign relates to the $C'\,^1\Delta$ and the "$+$" to the $C\,^1\Sigma^+$ state; see also Table IV. The MRCI(+Q) bond distances are very similar, namely, 1.1981 (1.1967) $[C'\,^1\Delta]$ and 1.2132 (1.2138) $[C\,^1\Sigma^+]$ Å, in excellent agreement with experiment,[9] but their adiabatic dissociation energies differ considerably between each other, i.e., $D_e=89.6$ (89.7) and 63.7 (62.3) kcal/mol.

The $B\,^1\Sigma^+$ state corelates adiabatically to the first Rydberg state of $B(^2S^*;2s^23s^1)+H(^2S)$. It is intercepted by a $^1\Sigma^+$ state of ionic character $B^+(^1S)H^-(^1S)$, hence the double well shown in Fig. 1. As the ionic $^1\Sigma^+$ comes in, it creates avoided crossings with all six excited $^1\Sigma^+$ states and maintains its ionic character from infinity to about 4.0 a.u. where the last avoided crossing occurs with the $B\,^1\Sigma^+$ state. The depth of the first, ionic, minimum is 5.44 eV ($=125.5$ kcal/mol) with respect to the diabatic products $B^+(^1S)+H^-(^1S)$ at $r_e=3.02$ Å, and 1.46 eV ($=33.7$ kcal/mol) with respect to the adiabatic products $B(^2S^*)+H(^2S)$. The dipole moment at the first minimum is close to 10 D with a Mulliken charge separation of about $0.5e^-$. The hump height is $12-13$ kcal/mol, whereas the global minimum of the $B\,^1\Sigma^+$ state at $r_e=1.215$ Å corresponds to a $D_e=49.6$ kcal/mol. The experimental r_e, ω_e, and $T_e(B\,^1\Sigma^+-X\,^1\Sigma^+)$ numbers are in very good agreement with our MRCI values. A few words are needed for the bonding in the $B\,^1\Sigma^+$ state. According to Table IV the leading configuration is $|B\,^1\Sigma^+\rangle \approx 0.93|2\sigma^23\sigma^1\overline{4\sigma^1}\rangle$; the three σ molecular orbitals are

$$2\sigma \approx (0.81)2s^B + (0.37)2p_z^{\,B} + (0.69)1s^H,$$

$$3\sigma \approx (0.19)2s^B - (0.70)2p_z^{\,B} + (0.41)s^B_{\text{diff}},$$

$$4\sigma \approx (0.80)s^B_{\text{diff}} + (0.29)2p_z^{\,B} + (0.31)1s^H,$$

where the subscript "diff" refers to diffuse (augmented) functions. The orbitals above in conjunction with the Mulliken atomic distribution point to the following vbL bonding scheme.
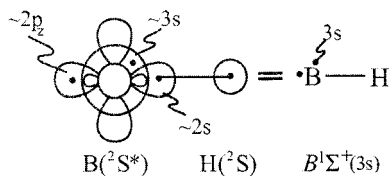
In other words, the 2σ is the bonding orbital, the 3σ is practically the $2p_z^{\,B}$ on boron, and the 4σ the Rydberg $3s^B$.

From a total of 32 calculated states we have discussed the first 11 up to the (repulsive) $1\,^5\Pi$ state; Table III. The remaining 21 states, all listed in Table III, consist of 17 states of Rydberg character, namely, $2\,^3\Sigma^+(3s)$ [the triplet companion of the $B\,^1\Sigma^+(3s)$], $[D\,^1\Pi, 3\,^3\Pi](3p)$, $[E\,^1\Sigma^+, 3\,^3\Sigma^+](3p)$, $[F\,^1\Sigma^+, 6\,^3\Sigma^+](3d)$, $[G\,^1\Pi, 4\,^3\Pi](3d)$, $[H\,^1\Delta, 1\,^3\Delta](3d)$, $[I\,^1\Sigma^+, 4\,^3\Sigma^+](4s)$, $[K\,^1\Pi, 5\,^3\Pi](4p)$, $[J\,^1\Sigma^+, 5\,^3\Sigma^+](4p)$, and four non-Rydberg states, $5\,^1\Pi, 6\,^3\Pi, 2\,^3\Delta, 7\,^3\Sigma^+$ stemming

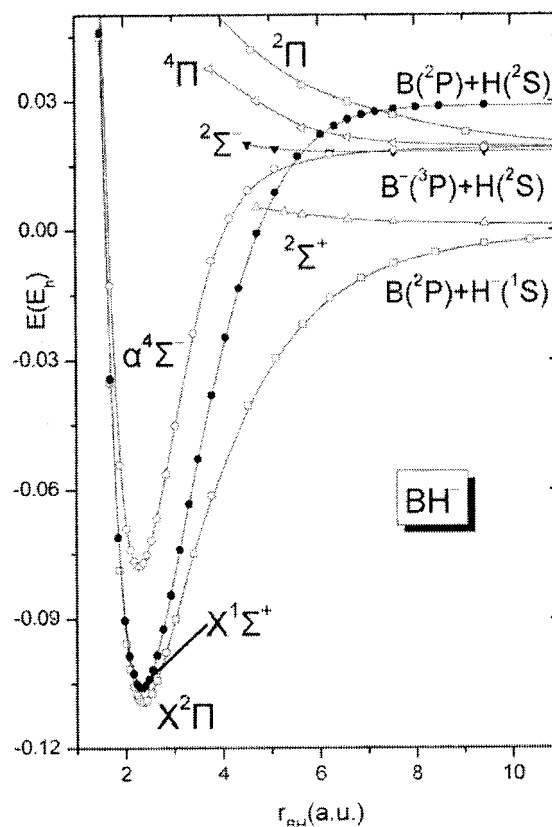FIG. 3. MRCI+Q/AC5Z potential energy curves of the BH$^-$ anion. The $X\,^1\Sigma^+$ state of BH is also included for comparison.

from the $B(^2D;2s^12p^2)+H(^2S)$ channel. The symbols in parenthesis, $3s$, $3p$, $3d$, $4s$, and $4p$, denote the symmetry defining Rydberg orbital on the B atom. The eight Rydberg singlets listed above have been detected experimentally and energy distances from the ground state (T_0) have been measured, as well as r_0 values for three of them (Table I). No experimental results are available for the companion triplet states. All experimental T_0 and r_0 values for these eight singlets are in remarkable agreement with our MRCI results, with the exception of the $K\,^1\Pi(4p)$ state where there is a discrepancy in T_0 by 3%. This agreement suggests that all our calculated numbers should be very reliable, either for the singlet or triplet Rydberg states.

From Table III it can be seen that the equilibrium bond lengths of all the 18 Rydberg states, singlets or triplets, are practically symmetry independent and very close to 1.20 Å due to the fact that all these states have the same type of bonding character as in the $B\,^1\Sigma^+(3s)$ previously described, with a Rydberg spectator electron whose angular momentum defines the symmetry of the state; see Table IV.

B. BH$^-$

Although the BH$^-$, isoelectronic to CH, has been observed experimentally since 1993,[23] experimental numbers are completely lacking from the literature. The ground state species $B(^2P)$, $H^-(^1S)$ and $B^-(^3P)$, $H(^2S)$ give rise to the molecular states $^2\Pi$, $^2\Sigma^+$ and $^{2,4}\Sigma^-$, $^{2,4}\Pi$, respectively. Their MRCI+Q/AC5Z PECs are given in Fig. 3 along with the MRCI+Q PEC of BH for reasons of comparison; Table V

TABLE V. Total energies E(hartree), equilibrium bond distances r_e(Å), dissociation energies D_e(kcal/mol), zero point energy ZPE(cm^{-1}), harmonic and anharmonic frequencies ω_e, and $\omega_e x_e$(cm^{-1}), rotational-vibrational constants a_e(cm^{-1}), ionization energy IE(eV), and the energy separation $a\,^4\Sigma^- - X\,^2\Pi$ T_e(cm^{-1}) of the anion ^{11}BH⁻. Results from the literature are also given for comparison. Basis set AC5Z/$_B$ A5Z/$_H$.

Method[a]	$-E$	r_e	D_e[b]	ZPE	ω_e	$\omega_e x_e$	a_e	1E	T_e
				$X\,^2\Pi$					
CASSCF	25.133 406	1.245	53.3					−1.48	0.0
MRCI	25.281 155	1.246	67.7	2.97	2119	59	0.53	−0.123	0.0
MRCI+Q	25.291 19	1.251	68.7	3.08	2170	66	0.53	0.085	0.0
RCCSD(T)	25.290 116	1.250	69.2	3.05	2159	61	0.51	0.081	0.0
RCCSDT	25.291 351	1.251	69.6					0.101	0.0
SCF[c]	25.106 221	1.2462			2262			−0.22	0.0
CEPA[d]		1.269			2082	66	0.52	0.03	0.0
MP4[e]	25.227 1	1.285	67.1		1997			0.07	0.0
MP4[f]	25.210 09	1.245			2275			0.12	0.0
FN-DMC[g]	25.279 8	1.269	70.0					0.11	0.0
				$a\,^4\Sigma^-$					
CASSCF	25.130 963	1.215	63.8	3.46		56	0.44		536
MRCI	25.253 854	1.200	62.7	3.59		57	0.44		5992
MRCI+Q	25.259 69	1.201	61.2	3.57		57	0.45		6914
RCCSD(T)	25.260 038	1.201	62.0	3.58		57	0.44		6601
RCCSDT	25.261 169	1.202	62.0						6624

[a]+Q refers to the Davidson correction.
[b]With respect to adiabatic fragments, i.e., $X\,^2\Pi \rightarrow B(^2P)+H^-(^1S)$ and $a\,^4\Sigma^- \rightarrow B^-(^3P)+H(^2S)$.
[c]Reference 24.
[d]Reference 25.
[e]Reference 26.
[f]Reference 27.
[g]Reference 28; equilibrium bond distance taken from Ref. 25.

shows numerical results of the states $X\,^2\Pi$ and $a\,^4\Sigma^-$. The adiabatic MRCI+Q [RCCSD(T)] (RCCSDT)/dAC5Z EA of BH (or the ionization energy of BH⁻) is, EA=0.085[0.081] (0.101) eV, in relative agreement with the FN-DMC value of 0.11 eV.[28] It is remarkable that at the MRCI/dAC5Z level, i.e., MRCI without the Davidson correction, the EA of BH is calculated to be −0.123 eV, in other words plainly wrong.

The ground state of BH⁻ is of $^2\Pi$ symmetry as in CH and well described at equilibrium by a single reference configuration, the leading CASSCF CF being $|X\,^2\Pi\rangle \approx 0.98|1\sigma^2 2\sigma^2 3\sigma^2 1\pi^1\rangle$. Obviously it correlates to $B(^2P)+H^-(^1S)$; recall that the EAs of B and H are 0.28 and 0.75 eV, respectively. The leading CF, the atomic Mulliken densities $2s^{1.45}\,2p_z^{1.28}\,2p_x^{1.00}\,2p_y^{0.06}\,3d^{0.09}/_B\,1s^{1.02}/_H$, and the repulsive nature of the next $^2\Pi$ state (Fig. 3) suggest the following bonding vbL diagram.

$B(^2P;M_L=\pm1)$ $H^-\,(^1S)$ $X\,^2\Pi$
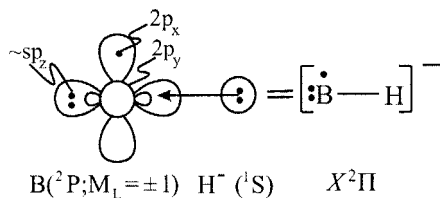
According to Mulliken populations, almost a whole electron is transferred from H⁻ to B, mainly to the empty $2p_z$ B orbital. The 3σ is a hybrid orbital extending on the back of the B atom and hosting two electrons, whereas the 2σ can be considered responsible for the bond; indeed the MRCI 2σ and 3σ natural orbitals are

$$2\sigma \approx (0.50)2s^B + (0.48)2p_z^{\,B} + (0.81)1s^H,$$

$$3\sigma \approx (0.73)2s^B - (0.47)2p_z^{\,B} - (0.19)1s^H.$$

Our recommended r_e and $D_e(D_0)$ values are 1.250 Å and 70(67) kcal/mol. The latter is in complete agreement with the FN-DMC result; see Table V.

The theoretical (experimental) D_e of the $X\,^2\Pi$ state of the isoelectronic CH molecule is 83.81(83.94) kcal/mol,[50] 14 kcal/mol larger than that of BH⁻. However, with respect to $B^-(^3P)+H(^2S)$, B⁻ being isoelectronic to $C(^3P)$, the binding energy of BH⁻ becomes 81 kcal/mol in agreement now with that of CH.

The $a\,^4\Sigma^-$ state of BH⁻ has never been studied before either experimentally or theoretically. At the RCCSDT level the $a\,^4\Sigma^- - X\,^2\Pi$ energy separation is 6624 cm^{-1} (=18.9 kcal/mol), much larger than the EA of BH, hence implying the transient nature of the $a\,^4\Sigma^-$ state of BH⁻. Recall that the $a\,^4\Sigma^- - X\,^2\Pi$ energy splitting of the isoelectronic CH species is 17.2 kcal/mol.[50] The leading MRCI configuration of the $a\,^4\Sigma^-$ and the atomic equilibrium distributions are $|a\,^4\Sigma^-\rangle \approx 0.99|1\sigma^2 2\sigma^2 3\sigma^1 1\pi_x^1 1\pi_y^1\rangle$ and $2s^{1.21}\,2p_z^{0.75}\,2p_x^{0.98}\,2p_y^{0.98}/_B\,1s^{0.97}/_H$, identical to the $a\,^4\Sigma^-$ state of CH.[50] Although the $a\,^4\Sigma^-$ state of BH⁻ adiabatically correlates to $B^-(^3P)+H(^2S)$, its interaction with a $a\,^4\Sigma^-$ state emanating from $B^-(^5S;2s^12p^3)+H(^2S)$ suggests, in accordance also to the configuration function and population analysis, the vbL diagram given below:
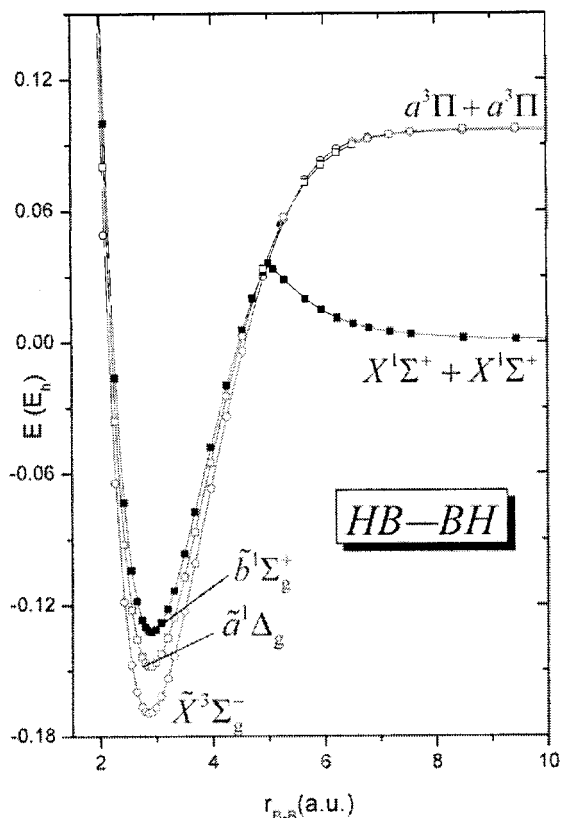
FIG. 4. MRCI/C5Z potential energy profiles with respect to B–B distance of the HBBH molecule. The B–H distance is optimized at every B–B bond length.
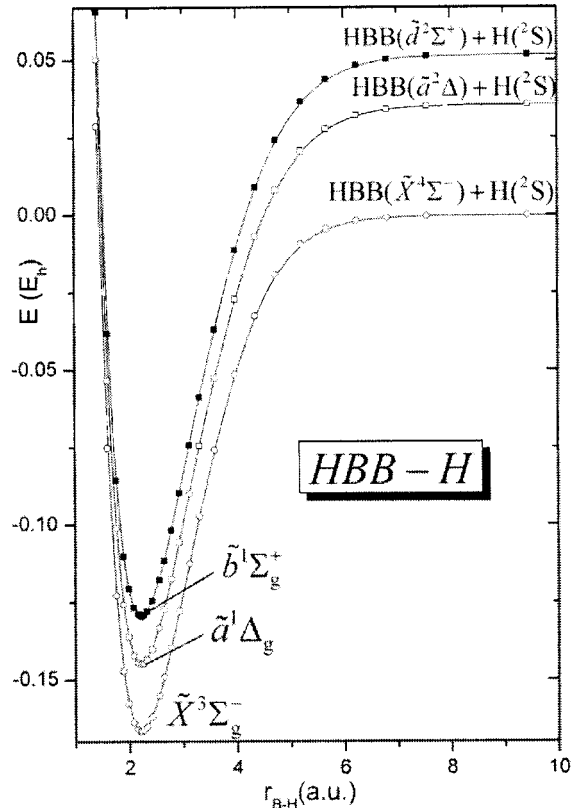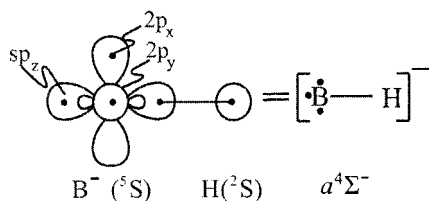

FIG. 5. MRCI/C5Z potential energy profiles with respect to HBB–H distance of the HBBH molecule. The H–B–BH bond distances are smoothly varied to match their final asymptotic values as a function of the HBB–H bond distance.

with

$$2\sigma \approx (0.64)2s^B + (0.36)2p_z^B + (0.75)1s^H,$$

$$3\sigma \approx (0.62)2s^B - (0.60)2p_z^H - (0.37)1s^H,$$

in agreement with the above scheme. The situation is completely analogous to the $a\,^4\Sigma^-$ state of CH.[50]

Numerical results for the $a\,^4\Sigma^-$ state are listed in Table V. Our recommended r_e and $D_e(D_0)$ values are 1.201 Å and 62.0(58.4) kcal/mol, respectively. Notice that going from the $X\,^2\Pi$ to the $a\,^4\Sigma^-$ state, the bond distance diminishes by 0.05 Å. It is interesting that in CH the corresponding bond length shortening is 0.03 Å, whereas its binding energy is $D_e = 66.2$ kcal/mol, remarkably similar figures to that of BH⁻. From Fig. 3 it is seen that the rest four states $^2\Sigma^+$ and $^2\Sigma^-$, $^4\Pi$, $^2\Pi$ correlating to $B(^2P)+H^-(^1S)$, and $B^-(^3P)+H(^2S)$ are purely repulsive. For the last three states, van der Waals minima have been detected at $6.80(^2\Sigma^-)$, $12.5(^4\Pi)$, and $16.8(^2\Pi)$ a.u. with interaction energies of 168, 13, and 11 cm⁻¹, respectively.

C. HBBH

The united atom corresponding to BH is the C atom, and of course, HBBH is isoelectronic to C_2. The leading MRCI configurations of the $X\,^1\Sigma_g^+$ state of C_2 are[51]

$$|X\,^1\Sigma_g^+\rangle \approx |1\sigma_g^2 1\sigma_u^2 2\sigma_g^2 [(0.84)2\sigma_u^2 - (0.37)3\sigma_g^2]1\pi_u^4\rangle,$$

which correspond to the following vbL diagram.
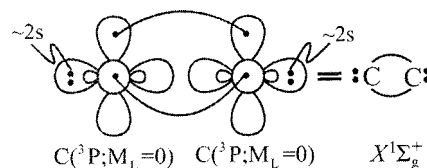
The second excited state of C_2, $|b\,^3\Sigma_g^-\rangle$ $\approx 0.97|1\sigma_g^2 1\sigma_u^2 2\sigma_g^2 2\sigma_u^2 3\sigma_g^2 1\pi_{u,x}^1 1\pi_{u,y}^1\rangle$, is located (experimentally) 6435.87 cm⁻¹ above the X-state,[51,52] and its bonding diagram is clearly as follows:
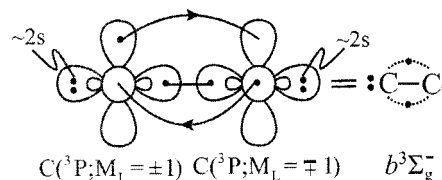
featuring a σ bond and two half π bonds. Two more low-lying states of C_2, the $B\,^1\Delta_g$ and $B'\,^1\Sigma_g^+$ are located (experi-

TABLE VI. Absolute energy values E (E_h), equilibrium HB–BH and H–BB–H bond distances r_e (B–B) and r_e (B–H) in Å, binding energies D_e and D_0 (kcal/mol), harmonic frequencies ω_e (cm^{-1}), and energy splittings of the first three electronic states of the linear H^{11}B^{11}BH molecule. Basis set C5Z/$_B$ 5Z/$_H$.

Property	$\widetilde{X}\,^3\Sigma_g^-$			$\widetilde{a}\,^1\Delta_g$		$\widetilde{b}\,^1\Sigma_g^+$	
	MRCI	MRCI+Q	RCCSD(T)	MRCI	MRCI+Q	MRCI	MRCI+Q
$-E$	50.737 27	50.748 75	50.748 10	50.715 48	50.728 11	50.700 07	50.712 01
r_e(HB–BH)	1.507 4	1.506 6	1.505 5	1.522 4	1.521 0	1.534 7	1.534
r_e(H–BB–H)	1.173 1	1.172 4	1.172 4	1.171 6	1.171 0	1.171 2	1.170 6
D_e(HB–BH)	168.6	170.0	169.5	154.9	157.0	85.4	85.7
D_0(HB–BH)	162.9	164.1	163.7	148.5	150.4	⋯	⋯
D_e(HBB–H)	104.6	106.2	105.6	113.4	114.7	113.8	115.1
D_0(HBB–H)	99.1	100.7	100.1	106.6	107.9	⋯	⋯
$\omega_e(\pi_g)^a$	571	568	582	799	820	640	645
$\omega_e(\pi_u)^b$	615	603	619	630	654	577	582
$\omega_e(\sigma_g)^c$	1249	1274	1261	1213	1211	1210	1211
$\omega_e(\sigma_u)^d$	2768	2793	2783	2784	2785	2773	2764
$\omega_e(\sigma_g)^e$	2806	2832	2821	2820	2821	2817	2819
T_e	0.0	0.0	0.0	4782	4531	8164	8064

[a]*trans* H–BB–H bending.
[b]*cis* H–BB–H bending.
[c]HB–BH stretching.
[d]H–BB–H antisymmetric stretching.
[e]H–BB–H symmetric stretching.

mentally) 12 082.3360 and 15 409.1390 cm^{-1} above the X-state,[52] respectively, and with configurations[51]
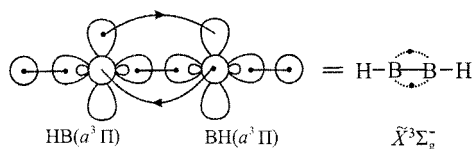
$$|B\,^1\Delta_g(-),B'\,^1\Sigma_g^-(+)\rangle \approx 0.68|1\sigma_g^2 1\sigma_u^2 2\sigma_g^2 2\sigma_u^2 3\sigma_g^2$$
$$\times[1\pi_{u,x}^2 \mp 1\pi_{u,y}^2]\rangle.$$

Obviously there is no way to form a stable linear HBBH molecule from two $X\,^1\Sigma^+$ states of BH. The analogous state to C(^3P) is the first excited state of BH, that is, $a\,^3\Pi$, 10 585 cm^{-1} above its X-state (*vide supra*). However, the ground state of HBBH is of $^3\Sigma_g^-$ symmetry[34,35] similar to the $b\,^3\Sigma_g^-$ state of C$_2$ and the first two excited states of symmetries $\widetilde{a}\,^1\Delta_g$ and $\widetilde{b}\,^1\Sigma_g^-$ similar to the excited states $B\,^1\Delta_g$ and $B'\,^1\Sigma_g^+$. Recall also that the first three states of O$_2$ are $X\,^3\Sigma_g^-$, $a\,^1\Delta_g$, and $b\,^1\Sigma_g^+$. The configuration of O(^3P) atom can be considered as complementary to that of the C(^3P) atom.

Presently we have examined the first three states of HBBH at high level of theory. In particular, for the $\widetilde{X}\,^3\Sigma_g^-$, $\widetilde{a}\,^1\Delta_g$, and $\widetilde{b}\,^1\Sigma_g^+$ states we have performed icMRCI and RCCSD(T) ($\widetilde{X}\,^3\Sigma_g^-$) calculations using a cc-pCV5Z/$_B$ cc-pV5Z/$_H$ basis set. Figures 4 and 5 display PECs with respect to HB–BH and HBB–H coordinates, respectively, whereas numerical results are presented in Table VI.
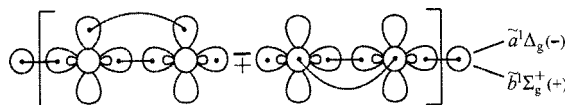
The leading MRCI CFs and vbL diagrams of the $\widetilde{X}\,^3\Sigma_g^-$, $\widetilde{a}\,^1\Delta_g$, and $\widetilde{b}\,^1\Sigma_g^+$ states are

$$|\widetilde{X}\,^3\Sigma_g^-\rangle \approx 0.97|1\sigma_g^2 1\sigma_u^2 2\sigma_g^2 2\sigma_u^2 3\sigma_g^2 1\pi_{u,x}^1 1\pi_{u,y}^1\rangle$$

and

$$|\widetilde{a}\,^1\Delta_x; b\,^1\Sigma_g^+\rangle \approx 0.68|1\sigma_g^2 1\sigma_u^2 2\sigma_g^2 2\sigma_u^2 3\sigma_g^2$$
$$\times(1\pi_{u,x}^2 \mp 1\pi_{u,y}^2)\rangle,$$

Notice that the coefficients "0.97" and "0.68" of the $\widetilde{X}\,^3\Sigma_g^-$ and $\widetilde{a}\,^1\Delta_g$, $\widetilde{b}\,^1\Sigma_g^+$ states are identical to those of the corresponding C$_2$ states, i.e., $b\,^3\Sigma_g^-$ and $B\,^1\Delta_g$, $B'\,^1\Sigma_g^+$.

The atomic Mulliken densities are, as expected, identical for all three states, namely, $2s^{1.12}\,2p_z^{0.80}\,2p_x^{0.48}\,2p_y^{0.48}/_B$ $1s^{1.01}/_H$. The HB–BH r_e and D_e (D_0) values with respect to two $a\,^3\Pi$ BH fragments are (Å, kcal/mol) 1.507, 170 (164) [$\widetilde{X}\,^3\Sigma_g^-$], 1.521, 157 (150) [$\widetilde{a}\,^1\Delta_g$], 1.534, 147 (140) [$\widetilde{b}\,^1\Sigma_g^+$]. A word of caution is required here; due to an avoided crossing at 4.91 a.u. with the $^1\Sigma_g^+$ repulsive state correlating to two $X\,^1\Sigma^+$ BH fragments, the binding energy of the $\widetilde{b}\,^1\Sigma_g^+$ state with respect to the ground state BH species is $D_e=85.7$ (80.9) kcal/mol; see Table VI and Fig. 4.

Referring to the work of Perić *et al.*,[35] total MRDCI energies are 150mE_h higher, bond distances 0.02 Å longer, and HB–BH dissociation energies (D_e) 8 kcal/mol smaller than ours.

Finally, the T_e splittings $\widetilde{a}\,^1\Delta_g$-$\widetilde{X}\,^3\Sigma_g^-$=4531 cm^{-1} and $\widetilde{b}\,^1\Sigma_g^+$-$\widetilde{a}\,^1\Delta_g$=3533 cm^{-1} follow the same pattern with the analogous C$_2$ (Ref. 52) and O$_2$ (Ref. 9) splittings (in cm^{-1}): $B\,^1\Delta_g$-$b\,^3\Sigma_g^-$=5646.5, $B'\,^1\Sigma_g^+$-$B\,^1\Delta_g$=3326.8, and $a\,^1\Delta_g$-$X\,^3\Sigma_g^-$=7918.1, $b\,^1\Sigma_g^+$-$a\,^1\Delta_g$=5277.0.

Stretching apart one of the two hydrogens of HBBH, one obtains the potential energy profiles shown in Fig. 5. The ground state of the HB$_2$ is linear (HBB) with a $^4\Sigma^-$ symmetry and a first excited state also linear and of $^2\Delta$ symmetry. According to Fig. 5 the first two states of HBBH, $\widetilde{X}\,^3\Sigma_g^-$ and

$\tilde{a}\ ^1\Delta_g$, correlate to the $\tilde{X}\ ^4\Sigma^-$ and $\tilde{a}\ ^2\Delta$ states of HBB, respectively. On the other hand, by stretching the H atom linearly, the $\tilde{b}\ ^1\Sigma_g^+$ state of HBBH correlates to $^2\Sigma^+$ (rather $\tilde{d}\ ^2\Sigma^+$) but the latter has one imaginary frequency. The $\tilde{d}\ ^2\Sigma^+$ was not examined any further, therefore the three HBB–H binding energies are reffered to the linear HBB fragments. The D_e (D_0) HBB–H values of $\tilde{X}\ ^3\Sigma_g^-$ and $\tilde{a}\ ^1\Delta_g$ states are 106 (100) and 115 (108) kcal/mol, respectively. For the $\tilde{b}\ ^1\Sigma_g^+$ state, D_e should be close to and rather smaller than 115 kcal/mol. Observe that the $\tilde{X}\ ^3\Sigma_g^-$ HBB–H D_e is by 21 kcal/mol larger than the D_e of the BH ($X\ ^1\Sigma^+$). *Mutatis-mutandis* the situation is similar to the binding energy (D_0) of HCC–H ($\tilde{X}\ ^1\Sigma_g^+$) versus C–H ($X\ ^2\Pi$), i.e., 131 (Ref. 53) and 79.9 kcal/mol.[9]

V. SUMMARY

We have examined the electronic structure and bonding character of the molecular systems BH, BH$^-$, and HBBH by multireference (CASSCF+1+2) and coupled-cluster [RCCSD(T) and RCCSDT] methods, using extensive correlation consistent basis sets. The core $1s^2$ electrons of the B atom have been correlated for all molecules examined; for this purpose core-tuned basis functions were included. We can claim that our results are the most accurate so far in the literature.

For the diatomic BH we have constructed complete PECs of 32 states adiabatically correlating to the first eight channels of B+H(^2S), spanning an energy range of about 10 eV. For all bound states we report common spectroscopic parameters (r_e, ω_e, $\omega_e x_e$, a_e, $\bar{D}_e$), binding energies (D_e or D_0), dipole moments (μ) calculated as expectation values ($\langle\mu\rangle$) and by the finite field approach (μ_{FF}), and energy separations (T_e). All calculated properties are in excellent agreement with available experimental results. 18 states are of Rydberg character, i.e., they correlate to a Rydberg state B atom ($2s^23s^1$, $2s^23p^1$, $2s^23d^1$, $2s^24s^1$, $2s^24p^1$). The ground state of BH is of $^1\Sigma^+$ symmetry with $D_0=81.43$ kcal/mol, a definitive value within a fraction of 1 kcal/mol. The dipole moments range widely from about -9 to $+8$ D, the positive direction being from B to H; $\mu(X\ ^1\Sigma^+)=+1.403$ D as contrasted to an experimental value of 1.27 ± 0.21 D. Dissociation energies range from 90 kcal/mol ($C'\ ^1\Delta$) to 2.50 kcal/mol ($1\ ^5\Sigma^-$), with bond distances from 1.190 Å ($a\ ^3\Pi$) to 1.93 Å ($2\ ^3\Pi$). In addition, the bond length of all Rydberg states is constant and very close to 1.20 Å, reflecting a bond character of the same nature. Finally, it should be stated, that for 25 states of BH theoretical results are reported for the first time, whereas experimental results on various properties exist for 13 singlets and two triplets ($a\ ^3\Pi, b\ ^3\Sigma^-$).

For the BH$^-$ anion, isoelectronic to CH, no experimental numbers exist. The ground state of BH$^-$ is of $^2\Pi$ symmetry with $D_0=67$ kcal/mol and ionization energy (or EA of BH) of 0.101 eV. The first excited state of BH$^-$, $a\ ^4\Sigma^-$, 18.9 kcal/mol higher than the X-state and therefore of metastable nature, correlates diabatically to B$^-(^5S)$+H(^2S) and is reported for the first time. For both states full PECs have been constructed.

For the linear HBBH system we have examined three states, namely, $\tilde{X}\ ^3\Sigma_g^-$, $\tilde{a}\ ^1\Delta_g$, and $\tilde{b}\ ^1\Sigma_g^+$ and the corresponding potential energy profiles with respect to two BH fragments. For the same states energy profiles have been calculated as well with respect to HBB+H. No experimental numbers exist for this system. Our results, energetics, geometries, and harmonic frequencies can be considered as the most reliable so far in the literature. The $\tilde{X}\ ^3\Sigma_g^-$, $\tilde{a}\ ^1\Delta_g$, and $\tilde{b}\ ^1\Sigma_g^+$ states are completely analogous to the $b\ ^3\Sigma_g^-$, $B\ ^1\Delta_g$, and $B'\ ^1\Sigma_g^+$ states of the isoelectronic species C$_2$, but their ordering follows that of the first three states of O$_2$.

We would like to believe that the present study sheds some light to the electronic structure of these complex systems and can also be helpful to future workers, particularly to the experimentalists.

ACKNOWLEDGMENTS

[1] E. J. Corey, Chem. Eng. News **81**, 40 (2003); see also H. Tang and S. Ismail-Beigi, Phys. Rev. Lett. **99**, 115501 (2007).

[2] See for instance, N. N. Greenwood and A. Earnshaw, *Chemistry of the Elements*, 2nd ed. (Butterworth-Heinemann, Oxford, 1998).

[3] W. Lochte-Holtgreven and E. S. van der Vleugel, Z. Phys. **70**, 188 (1931).

[4] G. Herzberg, *Molecular Spectra and Molecular Structure. I. Spectra of Diatomic Molecules* (van Nostrand, New York, 1950).

[5] F. S. Pianalto, L. C. O'Brien, P. C. Keller, and P. F. Bernath, J. Mol. Spectrosc. **129**, 348 (1988).

[6] J. Clark, M. Konopka, L.-M. Zhang, and E. R. Grant, Chem. Phys. Lett. **340**, 45 (2001).

[7] R. Thomson and F. W. Dalby, Can. J. Phys. **47**, 1155 (1981).

[8] C. R. Brazier, J. Mol. Spectrosc. **177**, 90 (1996).

[9] K. P. Huber and G. H. Herzberg, *Molecular Spectra and Molecular Structure. IV. Constants of Diatomic Molecules* (Van Nostrand Reinhold, New York, 1979).

[10] W. T. M. L. Fernando and P. F. Bernath, J. Mol. Spectrosc. **145**, 392 (1991).

[11] J. W. C. Johns, F. A. Grimm, and R. F. Porter, J. Mol. Spectrosc. **22**, 435 (1967).

[12] C. W. Bauschlicher, Jr., S. R. Langhoff, and P. R. Taylor, J. Chem. Phys. **93**, 502 (1990).

[13] R. C. Shani, J. Chem. Phys. **25**, 332 (1956).

[14] L. A. Curtiss and J. A. Pople, J. Chem. Phys. **90**, 2522 (1989).

[15] D. Feller, D. A. Dixon, and K. A. Peterson, J. Phys. Chem. A **102**, 7053 (1998).

[16] W.-T. Luh and W. C. Stwalley, J. Mol. Spectrosc. **145**, 200 (1991).

[17] L. A. Pederson, H. Hettema, and D. R. Yarkony, J. Phys. Chem. **98**, 11069 (1994), and references therein.

[18] See, for instance, (a) F. Grimaldi, A. Lecourt, H. Lefebvre-Brion, and C. M. Moser, J. Mol. Spectrosc. **20**, 341 (1966); (b) P. E. Cade and W. M. Huo, J. Chem. Phys. **47**, 614 (1967); (c) P. K. Pearson, C. F. Bender, and H. F. Schaefer III, *ibid.* **55**, 5235 (1971); (d) S. A. Houlden and I. G. Csizmadia, Theor. Chim. Acta **35**, 173 (1974); (e) R. J. Blint and W. A. Goddard III, Chem. Phys. **3**, 297 (1974); (f) R. Cimiraglia and M. Persico, J. Mol. Spectrosc. **87**, 303 (1981); (g) M. Jaszuński, B. O. Roos, and P.-O. Widmark, J. Chem. Phys. **75**, 306 (1981).

[19] L. Gagliardi, G. L. Bendazzoli, and S. Evangelisti, Mol. Phys. **91**, 861 (1997).

[20] C. E. Waltz, H.-W. Kim, and H. F. Hameka, Int. J. Quantum Chem. **17**, 479 (1980).

[21] G. T. Daborn and N. C. Handy, Mol. Phys. **49**, 1277 (1983).

[22] A. Halkier, H. Larsen, J. Olsen, P. Jørgensen, and J. Gauss, J. Chem. Phys. **110**, 734 (1999).

[23] C. J. Reid, Int. J. Mass Spectrom. Ion Process. **124**, R25 (1993).

[24] K. M. Griffing and J. Simons, J. Chem. Phys. **62**, 535 (1975).

[25] P. Rosmus and W. Meyer, J. Chem. Phys. **69**, 2745 (1978).

[26] G. Frenking and W. Koch, J. Chem. Phys. **84**, 3224 (1986).

[27] J. A. Pople, P. von R. Schleyer, J. Kaneti, and G. Spitznagel, Chem. Phys. Lett. **145**, 359 (1988).

[28] G. Morosi, M. Mella, and D. Bressanini, J. Chem. Phys. **111**, 6755 (1999).

[29] J. D. Dill, P. von R. Schleyer, and J. A. Pople, J. Am. Chem. Soc. **97**, 3402 (1975).

[30] C. Jouany, J. C. Barthelat, and J. P. Dauden, Chem. Phys. Lett. **136**, 52 (1987).

[31] M. Sana, G. Leroy, and Ch. Henriet, J. Mol. Struct. **187**, 233 (1989).

[32] G. Treboux and J.-C. Barthelat, J. Am. Chem. Soc. **115**, 4870 (1993).

[33] T. J. Tague, Jr. and L. Andrews, J. Am. Chem. Soc. **116**, 4970 (1994).

[34] L. B. Knight, K. Kerr, P. K. Miller, and C. A. Arrington, J. Phys. Chem. **99**, 16842 (1995).

[35] (a) M. Perić, B. Ostojić, and B. Engels, J. Mol. Spectrosc. **182**, 280 (1997); **182**, 295 (1997).

[36] R. J. Buenker and S. D. Peyerimhoff, Theor. Chim. Acta **35**, 33 (1974); **39**, 217 (1975).

[37] K. Raghavachari, G. W. Trucks, J. A. Pople, and M. Head-Gordon, Chem. Phys. Lett. **157**, 479 (1989); J. D. Watts, J. Gauss, and R. J. Bartlett, J. Chem. Phys. **98**, 8718 (1993); P. J. Knowles, C. Hampel, and H.-J. Werner, *ibid.* **99**, 5219 (1993); **112**, 3106E (2000).

[38] Y. Ralchenko, F.-C. Jou, D. E. Kelleher, A. E. Kramida, A. Musgrove, J. Reader, W. L. Wiese, and K. Olsen, 2007, NIST Atomic Spectra Database (version 3.1.3), (online). Available: http://physics.nist.gov/asd3 (29 November 2007). National Institute of Standards and Technology, Gaithersburg, MD.

[39] C. A. Moore, *Atomic Energy Levels*, Nat. Bur. Stand. (U.S.) Circ. No. 35 (U.S. GPO, Washington, D.C., 1971).

[40] T. H. Dunning, Jr., J. Chem. Phys. **90**, 1007 (1985).

[41] D. E. Woon and T. H. Dunning, Jr., J. Chem. Phys. **103**, 4572 (1995).

[42] R. A. Kendall, T. H. Dunning, Jr., and R. J. Harrison, J. Chem. Phys. **96**, 6796 (1992); **100**, 2975 (1994).

[43] H.-J. Werner, P. J. Knowles, R. Lindh *et al.*, MOLPRO, version 2006.1, a package of *ab initio* programs, see http://www.molpro.net.

[44] MRCC, a string-based quantum chemical program suite written by M. Kállay. See also M. Kállay, P. R. Surján, J. Chem. Phys. **115**, 2945 (2001), as well as www.mrcc.hu.

[45] M. Scheer, R. C. Bilodeau, and H. K. Haugen, Phys. Rev. Lett. **80**, 2562 (1998).

[46] C. Froese Fischer and G. Gaigalas, J. Phys. B **29**, 1169 (1996).

[47] D. H. Lee, W. D. Brandon, D. Hanstorp, and D. J. Pegg, Phys. Rev. A **53**, R633 (1996).

[48] K. R. Lykke, K. K. Murray, and W. C. Lineberger, Phys. Rev. A **43**, 6104 (1991).

[49] M. Douglas and N. M. Kroll, Ann. Phys. **82**, 89 (1974); B. A. Hess, Phys. Rev. A **32**, 756 (1985); **33**, 3742 (1986); G. Jansen and B. A. Hess, *ibid.* **39**, 6016 (1989).

[50] A. Kalemos, A. Mavridis, and A. Metropoulos, J. Chem. Phys. **111**, 9536 (1999).

[51] Unpublished results of this laboratory.

[52] M. Martin, J. Photochem. Photobiol., A **66**, 263 (1992).

[53] G. Herzberg, *Molecular Spectra and Molecular Structure. III. Electronic Spectra and Electronic Structure of Polyatomic Molecules* (van Nostrand, Florida, 1991).